

# A new time-gated synchronization controller for the detection of singlet oxygen luminescence

TONGQING HUANG<sup>†</sup>, DEFU CHEN<sup>†</sup>, WEIDA SU, HUIYUN LIN, BUHONG LI<sup>\*</sup>, SHUSEN XIE

Key Laboratory of OptoElectronic Science and Technology for Medicine of Ministry of Education, Fujian Provincial Key Laboratory for Photonics Technology, Fujian Normal University, Fuzhou 350007, P. R. China

<sup>†</sup> These authors contributed equally to this work.

A new time-gated synchronization controller is developed for the detection of near-infrared singlet oxygen ( $^1\text{O}_2$ ) luminescence around 1270 nm, in which the position and width of the sampling gate can be adjusted according to the time-resolved characteristics of  $^1\text{O}_2$  luminescence in different environments, respectively. Using this controller, the short-lived and long-lived background luminescence can be efficiently suppressed, which dramatically improves the signal-to-noise ratio for the measurement of time-integrated  $^1\text{O}_2$  luminescence. This new controller has the potential application for the detection of  $^1\text{O}_2$  luminescence.

(Received June 21, 2010; accepted August 12, 2010)

**Keywords:** Singlet oxygen, Luminescence, Detection, Time-gated synchronization controller, Signal-to-noise ratio

## 1. Introduction

Singlet oxygen ( $^1\text{O}_2$ ) is the lowest excited electronic state of molecular oxygen. This reactive form of oxygen plays an important role in a broad range of biological systems [1,2]. In particular,  $^1\text{O}_2$  has been widely regarded as the major cytotoxic agent in photodynamic therapy (PDT) [3]. With recent advances in the high sensitive near-infrared (NIR) photomultiplier tube (PMT) and photon counting techniques, the potential utility of the direct measurement of NIR  $^1\text{O}_2$  luminescence around 1270 nm as a dosimetric tool for PDT has received great attention [4,5]. The most attractive advantage of this direct photophysical technique for PDT dosimetry is that it can circumvent the complicated interactions between the photosensitizer, treatment light and molecular oxygen during the treatment [6].

Despite the challenges in detecting the extremely weak signal,  $^1\text{O}_2$  luminescence measurement has now been widely performed in both time- and spectrum-resolved experiments in cells *in vitro* and tissues *in vivo* [7-10]. As illustrated in Fig. 1, there is significant luminescence background in the early time points (1-2  $\mu\text{s}$ ) of the representative time-resolved  $^1\text{O}_2$  luminescence generated in aqueous environments, which affects the shape of the signal and changes the fit of the rise and decay times [11,12]. In addition, the luminescence emission beyond about 17  $\mu\text{s}$  is due to the longer-lived triplet state of the photosensitizers. In order to suppress the short-lived and long-lived luminescence and improve the signal-to-noise ratio (SNR) for the time-integrated  $^1\text{O}_2$  luminescence detection, a new time-gated synchronization controller (TGSC) with adjustable gate position and width is developed for the detection of  $^1\text{O}_2$  luminescence.

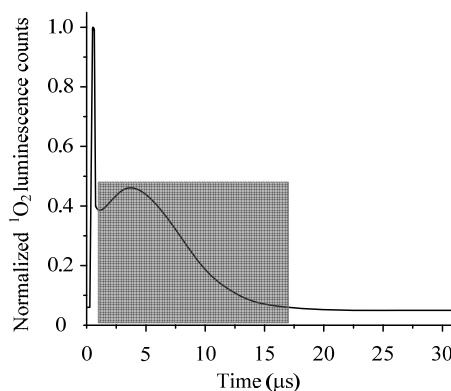


Fig. 1. Typical time-resolved  $^1\text{O}_2$  luminescence spectrum in aqueous environment

## 2. $^1\text{O}_2$ luminescence detection system

### 2.1 Time-gated synchronization controller

Fig. 2 illustrates the block diagram of the TGSC developed in this study. The clock generator is a crystal oscillation circuit that provides a highly stable output frequency at 10 MHz, and the corresponding clock period is 0.1  $\mu\text{s}$ . The clock signal is used to determine a time reference for the capture of data in the synchronous signal detection system. The sync counting unit consists of cascaded banks of sequential counters with self decoding function, and the unit is synchronously triggered by the external sync signal and used for counting the clock signal. In this controller, the start and stop signals for triggering the gate unit can be adjusted by the dial switches from 0 to 2.0  $\mu\text{s}$  and 0 to 20.0  $\mu\text{s}$  in 0.1  $\mu\text{s}$  steps, respectively, and

thus the position and width of the sampling gate for data acquirement are determined. The switch unit is controlled by the gate unit and is used to sample the desired input signal for detection.

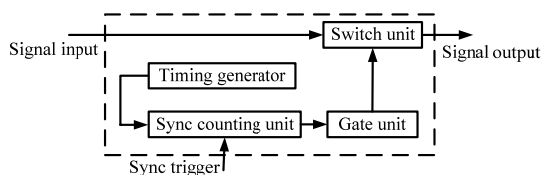


Fig. 2. Block diagram of TGSC.

## 2.2 $^1\text{O}_2$ luminescence detection system with TGSC

The detection system with TGSC used to measure spectrum-resolved  $^1\text{O}_2$  luminescence is shown schematically in Fig. 3. As for excitation light source, a diode-pumped, Q-switched, frequency-doubled Nd:YLF laser (QG-523-500; Crystalaser Inc., Reno, NV, USA) is used and emits at 523 nm. The excitation laser power can be adjusted by using a neutral-density attenuator. The solutions are placed in a standard 10 mm pathlength quartz cuvette (Yixing Jingke Optical Instrument Co., Ltd., Yixing, Jiangsu, China) mounted on a hotplate-stirrer unit (RH digital KT/C Package; IKA GmbH, Königswinter, Germany). This allows the solutions to be continuously stirred at a constant temperature of 25 °C and maintained the source-sample-detector geometry constant throughout the experiment. The cuvette is open so that the solutions are exposed to room air at the top. The sample is excited by the laser and the resultant NIR luminescence pass through the 1000 nm long-pass filter (Omega Optical, Brattleboro, VT, USA), the home-built optical collected unit and the 6 position motorized filter wheel (FW102B; Thorlabs Inc., Newton, NJ, USA). Five narrow-band filters centered at 1190, 1230, 1270, 1310 and 1350 nm (OD3 blocking, 20 nm FWHM; Omega Optical, Brattleboro, VT, USA) were sequentially mounted on the filter wheel in front of the PMT to sample the  $^1\text{O}_2$  luminescence spectrum.

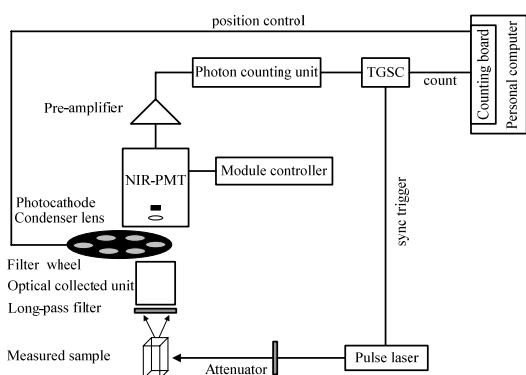


Fig. 3. Schematic diagram of the  $^1\text{O}_2$  luminescence detection system.

The collected NIR luminescence is detected by a PMT (H10330-45; Hamamatsu Corp., Hamamatsu, Japan) in the single photon counting mode. The PMT is contained in a thermally insulated, sealed-off housing evacuated to a high vacuum. The internal thermoelectric cooler eliminates the requirement for liquid nitrogen. The PMT output pulses is amplified by a wide bandwidth pre-amplifier (C6438; Hamamatsu Corp., Hamamatsu, Japan), and the pulse signals are discriminated and shaped to have a constant pulse width using a photon counting unit (C9744; Hamamatsu Corp., Hamamatsu, Japan). The newly developed TGSC is performed to remove the short-lived and long-lived background luminescence before the signals eventually recorded by a photon counting board (M8784; Hamamatsu Corp., Hamamatsu, Japan). The TGSC is triggered directly by the sync-out pulse from the laser. The control panel software of the detection system is written by LabVIEW 8.5 (National Instruments Corp., Austin, TX, USA), and operates on a personal computer. The measured data are then post processed with Origin 7.5 (OriginLab Corp., Northampton, MA, USA).

In order to collect the whole  $^1\text{O}_2$  luminescence in the solution-based and biological systems, the laser operates at a repetition rate of 12 kHz (the pulse width was approximately 25 ns) [4]. The corresponding energy of 1.67  $\mu\text{J}$  per pulse is obtained when the excitation power of the laser is kept to 20 mW. Based on the time-resolved characteristics of  $^1\text{O}_2$  luminescence in aqueous environments, the start and stop signals for triggering the gate unit in TGSC are set to 1.0  $\mu\text{s}$  and 17.0  $\mu\text{s}$  for measurements, respectively. The oscillograms of the laser trigger and the corresponding sampling gate of TGSC are measured using a digital storage oscilloscope (TDS1012; Tektronix Inc., Beaverton, OR, USA). As shown in Fig.4, the signal acquisition is started 1.0  $\mu\text{s}$  after the end of the excitation pulse and the sampling gate has the width of 16.0  $\mu\text{s}$  for data acquirement. Fig. 5 shows the timing diagram for the  $^1\text{O}_2$  luminescence detection system. The counter gate of the counting board is set to 100 ms, and therefore the  $^1\text{O}_2$  luminescence counts at each wavelength are summed over 1200 laser pulses. The operating voltage of the PMT is kept to  $-900$  V for the  $^1\text{O}_2$  luminescence measurements.

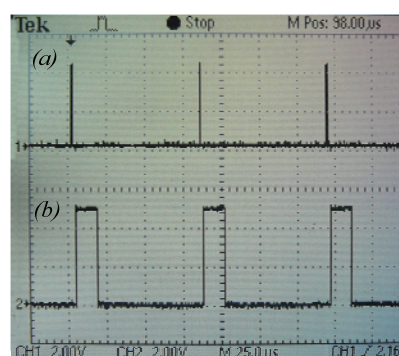


Fig. 4. The oscillograms of the (a) laser trigger and (b) sampling gate of TGSC.

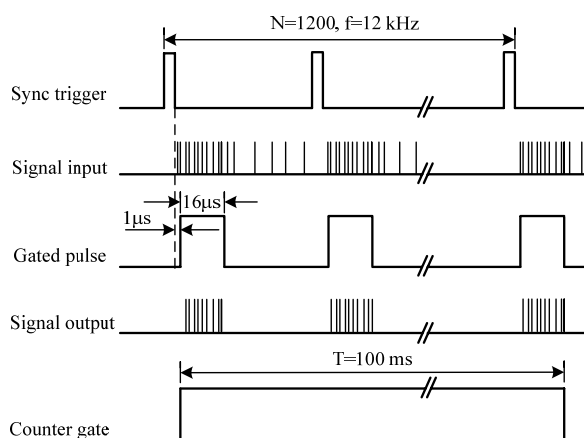


Fig. 5. Timing diagram of the  $^1\text{O}_2$  luminescence detection system.

### 3. Results and discussion

#### 3.1 $^1\text{O}_2$ luminescence measurement

The most common and available approach by which  $^1\text{O}_2$  can be generated is via photosensitization. In this study, Rose Bengal (RB) (Sigma-Aldrich., St. Louis, MO, USA) is chosen as a model photosensitizer in the solution-based measurements. The distilled-water is used to dilute RB at the final desired concentrations of 2.0, 3.0, 4.0 and 6.0  $\mu\text{M}$  for the following  $^1\text{O}_2$  luminescence measurements. Fig. 6 shows the time-integrated  $^1\text{O}_2$  luminescence signal as a function of the five individual wavelengths for various RB concentrations, in which the signals are measured by the  $^1\text{O}_2$  luminescence detection system with TGSC or without TGSC, respectively. Both spectra have a peak at 1270 nm indicating that the  $^1\text{O}_2$  luminescence emissions were captured, as expected. As can be seen in Fig. 6, the background luminescence is almost the same for both 1230 nm and 1310 nm filters in each case. However, the background luminescence for the detection system using TGSC is dramatically decreased in Fig. 6(a), which implies that the unwanted background luminescence has been efficiently suppressed, as compared to the measurements without TGSC in Fig. 6(b).

In order to determine the total  $^1\text{O}_2$  luminescence counts, the 1230 nm filter, which lies outside the  $^1\text{O}_2$  emission band, is treated as the luminescence background in the 1270 nm region, including the photosensitizer fluorescence and phosphorescence and fluorescence from optical components in the detection system.

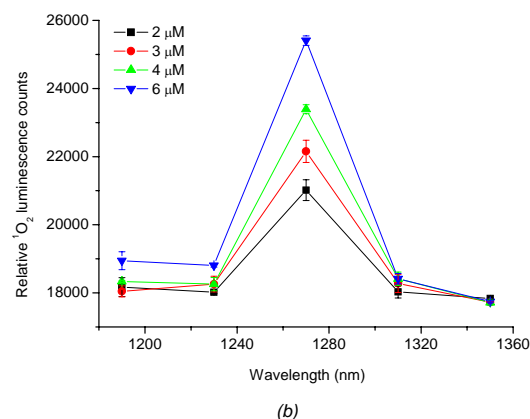
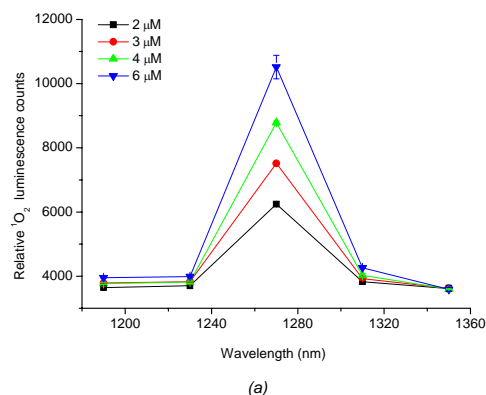


Fig. 6. The relative  $^1\text{O}_2$  luminescence counts as a function of wavelengths. The signals were measured by the  $^1\text{O}_2$  luminescence detection system (a) with TGSC and (b) without TGSC.

The total  $^1\text{O}_2$  luminescence counts for each measured sample is corrected for background by subtracting the control 1230 nm filter, and the total  $^1\text{O}_2$  luminescence counts (i.e., magnitude of the 1270 nm peak) can be determined as following:

$$I_{1\text{o}_2} = I_{1270} - I_{1230} \quad (1)$$

where  $I_{1270}$  and  $I_{1230}$  are the relative luminescence counts with 1270 and 1230 nm filters for each measured sample. The total  $^1\text{O}_2$  luminescence counts as a function of the RB concentrations are shown in Fig. 7. It can be seen that more than 94.2 percent of the  $^1\text{O}_2$  luminescence has been acquired by the system with TGSC, as expected.

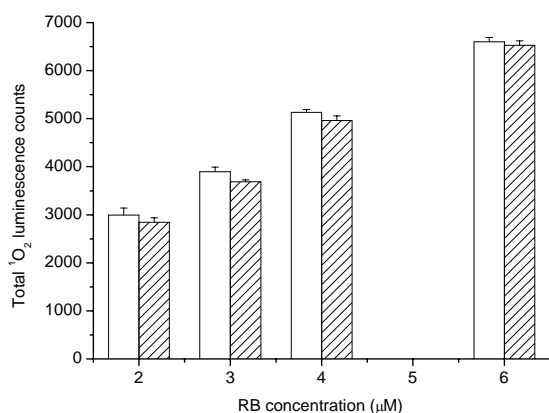


Fig. 7. Plot of the total <sup>1</sup>O<sub>2</sub> luminescence counts against the RB concentrations. The signals were measured by the <sup>1</sup>O<sub>2</sub> luminescence detection system with (▨) and without (□) TGSC.

### 3.2 SNR of the <sup>1</sup>O<sub>2</sub> luminescence detection system

As an additional attempt to demonstrate the performance of the <sup>1</sup>O<sub>2</sub> luminescence detection system with TGSC, the SNR for the detection system is further evaluated. As described in previous studies [13,14], we can define the SNR as the ratio between the maximum peak counts and the background counts, and the SNR is given by:

$$SNR = \frac{N_s}{\sqrt{N_s + 2N_b}} \quad (2)$$

where the signal counts ( $N_s$ ) is the total <sup>1</sup>O<sub>2</sub> luminescence counts at 1270 nm after background subtraction, and the background noise count ( $N_b$ ) is the luminescence counts from the control 1230 nm filter. Based on this assumption, the SNR of the <sup>1</sup>O<sub>2</sub> luminescence detection system with or without TGSC can be quantitatively calculated, respectively. As shown in Fig. 8, the SNR of the detection system by using TGSC is dramatically improved for various RB concentrations, as compared to the detection system without TGSC. However, it should be noted that the SNR varies as a function of the number of independent laser pulses that employed for each wavelength, and the SNR can be further improved with the increase of the number of excitation laser pulses [1].

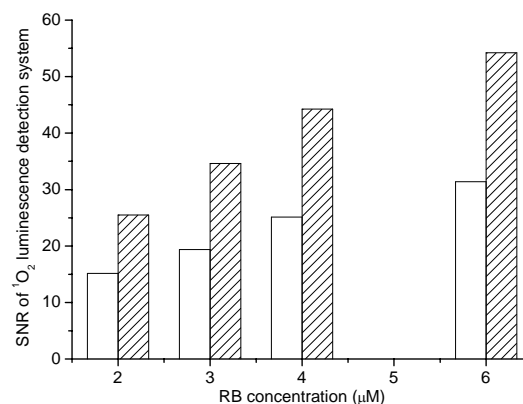


Fig. 8. Plot of the SNR against the RB concentrations with (▨) and without (□) TGSC.

## 4. Conclusions

A new TGSC with adjustable gate position and width was developed for the detection of <sup>1</sup>O<sub>2</sub> luminescence. Based on the characteristics of time-resolved <sup>1</sup>O<sub>2</sub> luminescence in the aqueous environment, the start and stop signals for triggering the gate unit in TGSC were set to 1.0 μs and 17.0 μs, respectively. The obtained results indicated that the <sup>1</sup>O<sub>2</sub> luminescence detection system with TGSC can not only efficiently capture the <sup>1</sup>O<sub>2</sub> luminescence, but also dramatically improve the SNR by suppressing the short-lived and long-lived background luminescence. Moreover, with this new TGSC, <sup>1</sup>O<sub>2</sub> luminescence in different environments can be measured by varying the position and width of the sampling gate, which is particularly useful for the detection of time-integrated <sup>1</sup>O<sub>2</sub> luminescence.

## Acknowledgements

This work was supported by the National Natural Science Foundation of China (60978070), the program for New Century Excellent Talents in University of China (NCET-10-0012), the Key Grant of Chinese Ministry of Education (209063), the Fujian Provincial Natural Science Foundation (2008J0001) and the Research Program of Fujian Provincial Educational Department (JA08031).

## References

- [1] E. Skovsen, J. W. Snyder, P. R. Ogilby, *Photochem. Photobiol.* **82**, 1187 (2006).
- [2] S. M. Driever, M. J. Fryer, P. M. Mullineaux, N. R. Baker, *Methods Mol. Biol.* **479**, 109 (2009).
- [3] K. R. Weishaupt, C. J. Gomer, T. J. Dougherty, *Cancer Res.* **36**, 2326 (1976).
- [4] A. Jimenez-Banzo, X. Ragas, P. Kapusta, S. Nonell,

- Photochem. Photobiol. Sci. **7**, 1003 (2008).
- [5] J. Schlothauer, S. Hackbarth, B. Roder, *Laser Phys. Lett.* **6**, 216 (2009).
- [6] M. Niedre, M. S. Patterson, B. C. Wilson, *Photochem. Photobiol.* **75**, 382 (2002).
- [7] M. J. Niedre, A. J. Secord, M. S. Patterson, B. C. Wilson, *Cancer Res.* **63**, 7986 (2003).
- [8] H. J. Laubach, S. K. Chang, S. Lee, I. Rizvi, D. Zurakowski, S. J. Davis, C. R. Taylor, T. Hasan, *J. Biomed. Opt.* **13**, 050504 (2008).
- [9] A. Jimenez-Banzo, M.L. Sagrista, M. Mora, S. Nonell, *Free Radic. Biol. Med.* **44**, 1926 (2008).
- [10] S. Hackbarth, J. Schlothauer, A. Preuss, B. Roder, *J. Photochem. Photobiol. B.* **98**, 173 (2010).
- [11] M. T. Jarvi, M. J. Niedre, M. S. Patterson, B. C. Wilson, *Photochem. Photobiol.* **82**, 1198 (2006).
- [12] J. Regensburger, T. Maisch, A. Felgentrager, F. Santarelli, W. Baumler, *J. Biophotonics.* **3**, 319 (2010).
- [13] S. Pellegrini, G. Buller, J. Smith, A. Wallace, S. Cova, *Meas. Sci. Technol.* **11**, 712 (2000).
- [14] Instruction Manual for the Photon Counting Unit Model C9744, Hamamatsu Corp., Hamamatsu, Japan.

---

\*Corresponding author: bhli@fjnu.edu.cn